Development 133, 237-250 doi:10.1242/dev.02188

XCR2, one of three *Xenopus* EGF-CFC genes, has a distinct role in the regulation of left-right patterning

Yasuko Onuma[1], Chang-Yeol Yeo[2] and Malcolm Whitman[1,*]

Members of the EGF-CFC family facilitate signaling by a subset of TGFβ superfamily ligands that includes the nodal-related factors and GDF1/VG1. Studies in mouse, zebrafish, and chick point to an essential role for EGF-CFC proteins in the action of nodal/GDF1 signals in the early establishment of the mesendoderm and later visceral left-right patterning. Antisense knockdown of the only known frog EGF-CFC factor (FRL1), however, has argued against an essential role for this factor in nodal/GDF1 signaling. To address this apparent paradox, we have identified two additional *Xenopus* EGF-CFC family members. The three *Xenopus* EGF-CFC factors show distinct patterns of expression. We have examined the role of *XCR2*, the only *Xenopus* EGF-CFC factor expressed in post-gastrula embryos, in embryogenesis. Antisense morpholino oligonucleotide-mediated depletion of *XCR2* disrupts left-right asymmetry of the heart and gut. Although *XCR2* is expressed bilaterally at neurula stage, *XCR2* is required on the left side, but not the right side, for normal left-right patterning. Left-side expression of *XNR1* in the lateral plate mesoderm depends on *XCR2*, whereas posterior bilateral expression of *XNR1* does not, suggesting that distinct mechanisms maintain *XNR1* expression in different regions of neurula-tailbud embryos. Ectopic XCR2 on the right side initiates premature right-side expression of XNR1 and XATV, and can reverse visceral patterning. This activity of XCR2 depends on its co-receptor function. These observations indicate that XCR2 has a crucial limiting role in maintaining a bistable asymmetry in nodal family signaling across the left-right axis.

KEY WORDS: EGF-CFC factor, *Nodal*, Left-right patterning, *Cripto*, *XCR*, *Xenopus*

INTRODUCTION

Members of the EGF-CFC gene family encode small extracellular glycosylated proteins, and include *Cripto* and *Cryptic* in humans and mouse (Bamford et al., 2000; Ciccodicola et al., 1989; Dono et al., 1991; Dono et al., 1993; Shen et al., 1997), *FRL1* in frogs (Kinoshita et al., 1995), *one-eyed pinhead*, *oep*, in zebrafish (Zhang et al., 1998) and *Cripto/CFC* in chick (Colas and Schoenwolf, 2000; Schlange et al., 2001). EGF-CFC family members share two conserved domains: an EGF-like domain and a CFC domain, which are conserved only among EGF-CFC family members (reviewed by Adamson et al., 2002; Minchiotti et al., 2002; Saloman et al., 2000; Shen and Schier, 2000). Recent genetic and biochemical studies have demonstrated that EGF-CFC proteins act as essential co-factors for signaling by the nodal/GDF1 subset of TGFβ superfamily ligands (reviewed by Saloman et al., 2000; Schier, 2003). EGF-CFC proteins facilitate the association of nodal and GDF1/VG1 ligands with Type I and Type II transmembrane receptors (Cheng et al., 2003; Reissmann et al., 2001; Yan et al., 2002; Yeo and Whitman, 2001). The EGF-like domain mediates association with nodal ligands, whereas the CFC domain interacts with the receptor complex. Loss-of-function studies have established that EGF-CFC proteins function as co-factors for nodal/GDF1 signals in both mesendoderm and left-right axis specification (Bamford et al., 2000; Ding et al., 1998; Gaio et al., 1999; Gritsman et al., 1999; Linask et al., 2003; Schlange et al., 2001; Xu et al., 1999; Yan et al., 1999).

The only reported frog EGF-CFC family member, *FRL1*, was originally identified in a screen for FGF receptor ligands (Kinoshita et al., 1995). Ectopic expression and antisense oligonucleotide studies have indicated that *FRL1* is essential for the activation of ERK and subsequently for neural formation (Yabe et al., 2003), and is also an essential co-factor for the dorsal determinant WNT11 (Tao et al., 2005). Strikingly, however, no defects in either the transduction of nodal/GDF1 signals or left-right patterning were observed following *FRL1* depletion, suggesting that the function of FRL1 might differ from that of EGF-CFC factors in other vertebrate model organisms. We report here the identification of two additional EGF-CFC family members in *Xenopus*. The three frog EGF-CFC factors show distinct spatial and temporal expression patterns during development. We have examined the effects of both loss and gain of function of one of these factors, *XCR2*, and have found that it is specifically required for normal left-right patterning of *XNR1* and *XATV* expression, and for visceral asymmetry. *XCR2* is expressed bilaterally at neurula-tailbud stages, but is required only on the left side for normal patterning. The requirement of *XCR2* for left-side-specific expression of the nodal-related gene *XNR1*, is consistent with prior work demonstrating that the expression of *nodal-related* ligands are maintained by a FAST1/FOXH1-mediated positive-feedback loop (Adachi et al., 1999; Norris et al., 2002; Osada et al., 2000; Saijoh et al., 2000). In addition, we found that ectopic expression of *XCR2* on the right side is sufficient to reverse left-right polarity, and this effect requires *XCR2* activity as a co-receptor for nodal/GDF1 ligands. These observations indicate not only that *XCR2* is required for nodal signaling during left-right patterning, but also that limitation of nodal signaling across the left-right axis by XCR2 can determine the polarity of the nodal gradient across this axis.

[1]Department of Developmental Biology, Harvard School of Dental Medicine, 188 Longwood Avenue, Boston, MA 02115, USA. [2]Department of Life Sciences and Center for Cell Signaling Research, Ewha Women's University, Seoul 120-750, Korea.

*Author for correspondence (e-mail: mwhitman@hms.harvard.edu)

Accepted 27 October 2005

MATERIALS AND METHODS

Plasmid construction, genomic cloning and design of antisense morpholino oligonucleotides

Using the BLAST search algorithm (Altschul et al., 1990), we identified EST clones corresponding to two novel *Xenopus laevis* EGF-CFC factors: (1) from the NIBB Mochii normalized *Xenopus laevis* neurula library, cDNA

clone XL044d20 (GenBank UniGene Xl. 15503); and (2) from the NICHD_XGC_Emb1 *Xenopus laevis* library, cDNA clone IMAGE Consortium CloneID 6864330 (GenBank CA987644). We designated these novel EGF-CFC factors *XCR2* and *XCR3S* (short form), respectively.

To generate pCS-XCR2, pCS2-XCR3S, pCS2-hCFC1, pCRII-XNR1 and pCRII-XATV, the ORF region of each EST clone (XCR2 or XCR3S) or cDNA insert of pSP64PA-humanCFC1 (Bamford et al., 2000), pCS2+XNR1 (Lustig et al., 1996) or pCS2+*XATV* (Cheng et al., 2000) was subcloned into pCS4+, a derivative of pCS2+ described by Yeo and Whitman (Yeo and Whitman, 2001), into the pCS2+ vector or into the pCRII vector (Invitrogen). To generate pCS2-XCR3L (long form), the ORF region of XCR3L was amplified by PCR from cDNA of stage 10.5 embryos, and subcloned into the pCS2+ vector. pCS-XCR2 mEGF (mutated EGF) and pCS-XCR2 mCFC (mutated CFC) were generated by PCR-based subcloning: Asn93 and Thr96 to Gly93 and Ala96 in XCR2 mEGF1, and His129 and Trp132 to Gly129 and Gly132 in XCR2 mCFC. All constructs generated by PCR amplification were sequence verified.

Xenopus laevis genomic clones of *XCR2* were isolated by PCR using the following primers: up (5′-AAGCAATTTCACATCAAC-3′) and down (5′-GGTGGGCCCCGCTGCCTCTAATG-3′; the linker sequence is underlined). A splice-site-targeted antisense morpholino oligonucleotide, TACACTCACTGTTAGTTCTTACCTC (XCR2 MO; 25-mer, underlined sequence is the region in the intron), was designed against the consensus sequence at the first exon-intron boundary derived from the sequence of two distinct *XCR2* genomic clones. A standard control morpholino oligo (SC MO) from GeneTools was used as a control.

Cell culture and luciferase assays

Plasmids used for transfection were: pCS2+XNR1 (Lustig et al., 1996); derrière/CS2+ (Sun et al., 1999); pCS-mouse nodal and pCS-mouse Cripto-3Flag (Yeo and Whitman, 2001); pCS-XCR2-3Flag that was generated by PCR-based subcloning and includes three repeats of the Flag epitope fused after Val191 of XCR2 in pCS-XCR2; pCS2-6Myc-mouse FAST1 (FOXH1) (Weisberg et al., 1998); Mix.2 ARE A3-lux (Chen et al., 1996); and pcDNA3.1/V5-His-TOPO/lacZ (Invitrogen). Human embryonic kidney 293T cells were cultured in 5% CO_2 at 37°C in DMEM supplemented with 10% FBS, 100 U/ml of penicillin and 100 μg/ml of streptomycin. Transient transfection assays were performed by the calcium phosphate method in triplicate (Sambrook and Russell, 2001). Plasmid mixtures contained 200 ng of each expression construct, 200 ng of the luciferase reporter plasmid, 80 ng of CMV-β-gal plasmid, and various amounts of pCS2+ vector to maintain a constant amount of total DNA. β-gal activity was confirmed to vary linearly with the quantity of plasmid transfected. Luciferase activity was measured 48 hours post-transfection and was normalized to the activity of co-transfected β-galactosidase activity. The fold differences in luciferase activity were calculated using the luciferase activity of the pCS2-6Myc-mouse FAST1 (FAST1) transfected control as basal level activity. Expression of each epitope-tagged protein was confirmed by western blotting.

Microinjection, immunohistochemistry and in situ hybridization analyses

Xenopus laevis embryos were obtained by artificial fertilization, and embryos were staged according to Nieuwkoop and Faber (Nieuwkoop and Faber, 1956). Synthetic *EGFP* mRNA was made using SP6 mMESSAGE mMACHINE (Ambion), and was co-injected with XCR2 MO and/or various plasmids into the marginal region of one blastomere of two-cell-stage embryos. Embryos were sorted into left- or right- injected groups based on EGFP-fluorescence, and then fixed for in situ hybridization analysis, or scored for heart and gut morphology at stage 45-46 according to Branford et al. (Branford et al., 2000).

In situ hybridization analyses were performed according to Sive et al. (Sive et al., 2000), but with the addition of 0.3% CHAPS in 2×SCC and 0.2×SSC for probe washing. In Fig. 6I,K-V, Fig. 7C,D and Fig. 8A-K,M-Q, hybridization and wash steps were performed at 70°C. RNA probes were synthesized from pCRII-XNR1 and pCRII-XATV. After staining, pigmented embryos were bleached and cleared. Immunohistochemistry was carried out according to Faure et al. (Faure et al., 2000) and Lee et al. (Lee et al., 2001). The sarcomere myosin-specific antibody MF 20 was provided by the Developmental Studies Hybridoma Bank at the University of Iowa. The signal was detected with AlexaFluor594 donkey anti-mouse IgG (H+L) antibody (Molecular Probes), or with peroxidase-conjugated donkey anti-mouse IgG (H+L) antibody (Jackson ImmunoResearch), and the DAB Substrate Kit (Vector Laboratories).

Semi-quantitative RT-PCR analysis

Extraction of total RNA and reverse transcription were performed according to Watanabe and Whitman (Watanabe and Whitman, 1999). *Ornithine decarboxylase* (*ODC*) was used as an internal control. Reverse transcriptase negative (RT–) reactions were carried against all samples using *ODC* primers to confirm the absence of genomic DNA contamination. Primers used for PCR were: *FRL1/XCR1* (up, 5′-CTGGTTTTTGCTAAGGACAC-3′; down, 5′-TTGCAATGCTTGATAAAATG-3′); for temporal expression analysis of *XCR2* (up, 5′-GCTGCGCATATGGGGTTCTT-3′; down, 5′-CGATAATGCAGCCTTGTTTTCTCT-3′); for RNA splicing analysis of *XCR2* (up, 5′-GCCCTTGGGATCCTTACATT-3′; down, 5′-GAGTCAA-TGTTATAAATATGAAT-3′); *XCR3* (up, 5′-GCTGTAATTCGCTTGG-GAAC-3′; down, 5′-TTTTGGACATGCACAGAAGC-3′); *VG1* (up, 5′-GACCGCTAACGATGAGTG-3′; down, 5′-AGGAATGTCTTCTGGCTC-3′); *XNR1* (Lustig et al., 1996); *ODC* (http://www.xenbase.org/). PCR

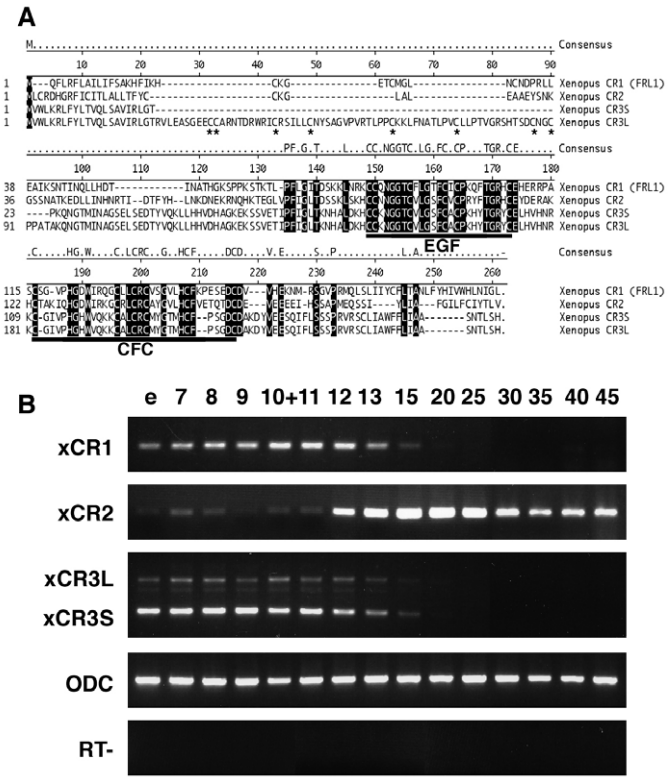

Fig. 1. Comparison of amino acid sequences and temporal expression patterns of *Xenopus* EGF-CFC factors. (**A**) Comparison of the amino acid sequences of *Xenopus* EGF-CFC proteins (XCR1, XCR2, XCR3S and XCR3L). XCR3L has a 72 amino acid insertion following the signal sequence of XCR3S. Dash indicates no amino acid present. Identical residues are shadowed. Conserved EGF-like domains and CFC domains are underlined. Cysteine residues in the additional 72 amino acids of XCR3L are indicated by asterisks. (**B**) Temporal expression patterns of *Xenopus* EGF-CFC genes (*XCR1*, *XCR2*, *XCR3S* and *XCR3L*) detected by RT-PCR. RNA was extracted from embryos at the stages indicated over each lane. *XCR3S* (lower band) and *XCR3L* (upper band) were detected using a set of primers designed to span the insert region. Both bands showed a similar temporal expression pattern. e, un-fertilized egg; RT-, RT-PCR reaction without reverse transcriptase.

products were separated by agarose gel electrophoresiss and visualized by ethidium bromide staining. PCR products of *XCR1* (*FRL1*), *XCR2*, *XCR3S* and *XCR3L* were recovered from gels and confirmed by sequencing.

RESULTS

Xenopus EGF-CFC factors are expressed in distinct patterns spatially and temporally

Because studies of the only reported *Xenopus* EGF-CFC factor, *FRL1*, suggested a functional difference from the proposed role of EGF-CFC factors in other vertebrate embryo model systems (Shen and Schier, 2000; Tao et al., 2005; Yabe et al., 2003), we searched the *X. laevis* EST database for additional EGF-CFC family members. Full sequencing of two EST clones of potential novel EGF-CFC family members identified these as two novel *Xenopus* EGF-CFC genes, *XCR2* and *XCR3* (Fig. 1A). The XCR2 and XCR3 proteins are 34.6% and 30.6% identical to FRL1, respectively, and 30.6% identical to each other. Examination of the *X. tropicalis* EST and genomic databases did reveal the existence of clear *X. tropicalis* orthologs for each of the *X. laevis* EGF-CFC genes (data not shown). While their overall sequences are quite divergent from one another, the three *X. laevis* EGF-CFC proteins share substantial conservation in the EGF-like and CFC domains, and all contain a putative *O*-linked fucosylation site, which has been identified in mammalian cripto as being crucial for function as a nodal co-receptor (Schiffer et al., 2001; Yan et al., 2002). The three *Xenopus* EGF-CFC proteins are nearly identical in size, with the notable exception being that the *XCR3* transcript occurs in two alternatively spliced forms; the longer form encodes 72 additional amino acids near the N terminus of the protein (Fig. 1A). This additional stretch is cysteine-rich but shows no homology to other known proteins or domains. The full-length sequences for *XCR2*, *XCR3S* (short form) and *XCR3L* (long form) have been submitted to GenBank under Accession Numbers AY796186, AY796188 and AY796189, respectively. *XCR2* and *XCR3* have also been identified independently by Dorey and Hill (K. Dorey and C. Hill, personal communication). To render the nomenclature for *Xenopus* EGF-CFC factors consistent we, Dorey and Hill, and the investigators who originally identified FRL1 (Kinoshita et al., 1995) (M. Kirschner, personal communication) propose to rename *FRL1* as *XCR1*.

To begin to characterize the developmental roles of *Xenopus* EGF-CFC factors, we examined the temporal expression patterns of *XCR1*, *XCR2* and *XCR3* by RT-PCR (Fig. 1B). Transcripts for all of the XCR genes were detected in unfertilized eggs, and *XCR1* and *XCR3* were expressed through early embryogenesis until the early neurula stage (stage 15). *XCR2* was expressed at very low levels maternally, expression increased markedly at the end of gastrulation (stage 12), and was maintained at high levels through tadpole stages (stage 45). *XCR3* was detected as two bands corresponding to the two splicing variants, *XCR3S* and *XCR3L*, which showed similar temporal expression patterns. *XCR1* and *XCR3* were expressed ubiquitously before gastrulation (Fig. 2A), whereas *XCR2* expression was too low to compare it in the different regions of the pre-gastrula embryo (not shown). We next examined the spatial expression patterns of the three *XCR* genes by in situ hybridization (Fig. 2). *XCR1* expression was strong in the entire prospective ectoderm at the beginning of gastrulation, and became restricted to the prospective neural plate by stage 12 (Fig. 2B,C), consistent with previous reports (Wessely et al., 2004; Yabe et al., 2003). *XCR3* was strongly expressed in the Organizer and the prospective endoderm at the onset of gastrulation (Fig. 2D). This expression became enriched anteriorly during gastrulation (Fig. 2E). *XCR2* was expressed at very low levels until stage 12, when its expression was detectable on the dorsal side (Fig. 2F). This dorsal expression was further restricted to the midline during neurulation (Fig. 2G), and in the notochord through

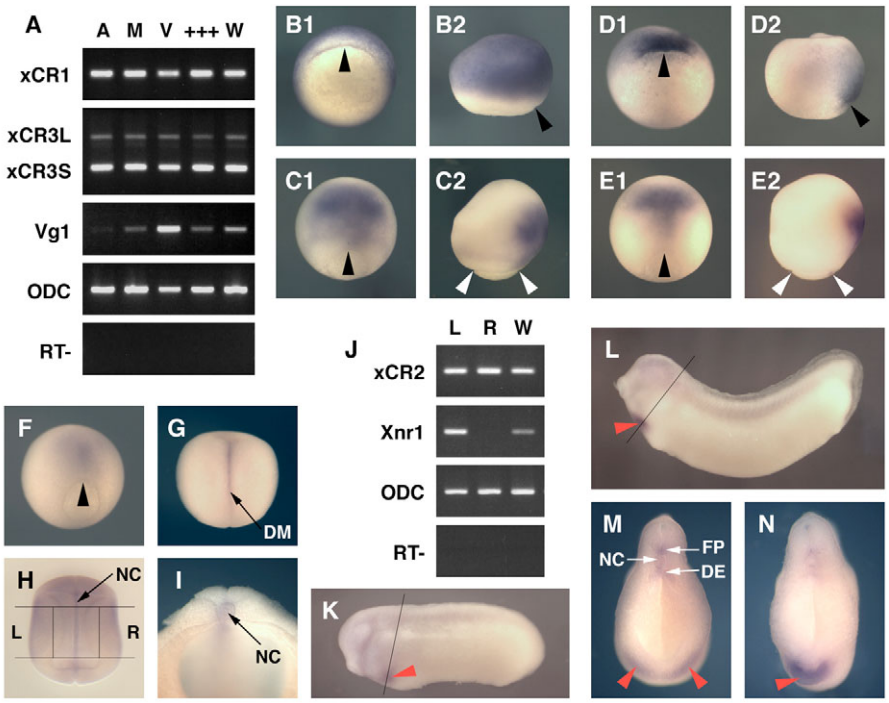

Fig. 2. Spatial expression patterns of *Xenopus* EGF-CFC genes. (**A**) Spatial expression patterns of *XCR1*, *XCR3S* and *XCR3L* at stage 9, as determined by RT-PCR of the animal region (A), the marginal region (M), the vegetal region (V), a mixture of the dissected three parts (+++) and intact whole embryos (W). *VG1* was used as a control for dissection. (**B-I**,**K-N**) Spatial expression analyses by in situ hybridization for *XCR1* (*FRL1*; B,C), *XCR3* (D,E) and *XCR2* (F-I,K-N). (B1,D1) Stage 10+ in vegetal view. The dorsal side is up. (C1,E1,F,G) Stage 12 (C,E,F) and stage 15 (G) in dorsal view. The anterior side is up. (B2,C2,D2,E2) Stage 10+ (B,D) and stage 12 (C,E) in lateral view. The anterior side is up and the dorsal side is to the right. (H) Stage 20 in dorsal view. Embryo was cleared with benzyl benzoate/benzyl alcohol. Lines show the left (L) and right (R) dissection model for RT-PCR (J). (I) Transverse bisected embryo at stage 20. (J) RT-PCR of the left lateral region (L), the right lateral region (R) and intact whole embryos (W) at stage 20. *XCR2* was expressed bilaterally, whereas *XNR1* was expressed on only the left side. (K) Stage 25. Line indicates the section plane shown in M. (L) Stage 30. Line indicates the section plane in N. (M,N) Transverse cut embryos at stage 25 (M) and stage 30 (N). Red arrowheads indicate the expression of *XCR2* in the prospective heart region; black arrowheads indicate the dorsal lip; white arrowheads indicate the blastopore. DE, dorsal endoderm; DM, dorsal midline; FP, floorplate; NC, notochord.

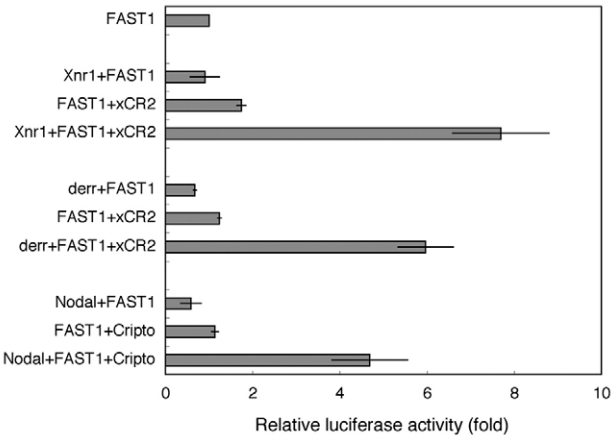

Fig. 3. XCR2 facilitates XNR1 and derrière signaling. 293T cells were transiently transfected with the A3-lux luciferase reporter. Luciferase activity was normalized to the activity of co-transfected β-galactosidase and then expressed as the fold difference in activity relative to that of FAST1 transfection. The average of three independent examinations in triplicate is shown. Error bars show s.d.

neurula stages (Fig. 2H,I). *XCR2* was also bilaterally expressed in the lateral plate region at stage 20 (Fig. 2H,J). *XCR2* was expressed in the prospective heart region at stage 25, and in the floor plate and dorsal endoderm in the dorsal midline (Fig. 2K,M). Dorsal midline expression decreased by stage 30, whereas the heart region expression was maintained (Fig. 2L,N). The markedly different temporal and spatial expression patterns of the XCR genes suggest that they have distinct developmental roles.

The distinctive expression pattern of *XCR2* suggested a role for *XCR2* that was distinct from those of *XCR1* and *XCR3*. We therefore examined whether *XCR2*, like other EGF-CFC factors, acts to facilitate nodal-like ligand signaling. The activity of *XCR2* on XNR1 or derrière signaling was tested in 293T cells transiently transfected with FAST1/FOXH1 and a nodal-responsive luciferase reporter, the Mix.2 ARE A3-luc reporter (Fig. 3). *XNR1* or *derrière* increase luciferase activity in a FOXH1-dependent manner, but only in the presence of co-transfected *XCR2*. Similar results were seen with co-transfection of the related mouse genes *Nodal* and *Cripto* (Fig. 3). These results indicate that *XCR2* can act as a co-factor for nodal-related ligands, as has been previously reported for other EGF-CFC factors. The fact that derrière signaling, as well as XNR1 signaling, is supported by XCR expression has not been reported, but is consistent with previous work showing that the structurally similar ligand VG1 requires EGF-CFC factors to signal, and that ectopic derrière shows only limited activity in zebrafish *MZoep* mutants (Cheng et al., 2003).

Left-side XCR2 expression is essential for left-right patterning

We next investigated the role of *XCR2* in early frog development using antisense morpholino oligonucleotide (MO)-mediated depletion. Because preliminary experiments indicated that two antisense MOs targeting *XCR2* translation were ineffective (data not shown), we designed an antisense MO targeting the first exon-intron junction to block *XCR2* pre-mRNA splicing. We cloned genomic DNA containing *XCR2* by PCR, and found the position of the first intron to be conserved with known EGF-CFC genes (data not shown, GenBank Accession Number AY796187) (Colas and Schoenwolf, 2000). A 25 nucleotide antisense MO was designed against the first exon-intron boundary; three bases targeted the first exon and 22 bases targeted the first intron (Fig. 4A,B). We first examined whether the XCR2 MO blocks endogenous RNA splicing by RT-PCR, using primers that span the first intron. In XCR2 MO-injected embryos, the amount of mature *XCR2* mRNA was decreased and an abnormal splicing variant was generated from a cryptic splice donor site (Fig. 4C). Correct splicing of *XCR2* was inhibited through stage 35. Splicing of *XCR2* mRNA was not affected by control MO injection. The abnormal splicing variant detected in *XCR2* MO-injected embryos has an in-frame termination codon immediately following the end of exon I, resulting in an eight amino acid long predicted coding sequence (Fig. 4B). These results indicate that this splice-site-targeted antisense MO is an effective tool for the inhibition of endogenous *XCR2* function.

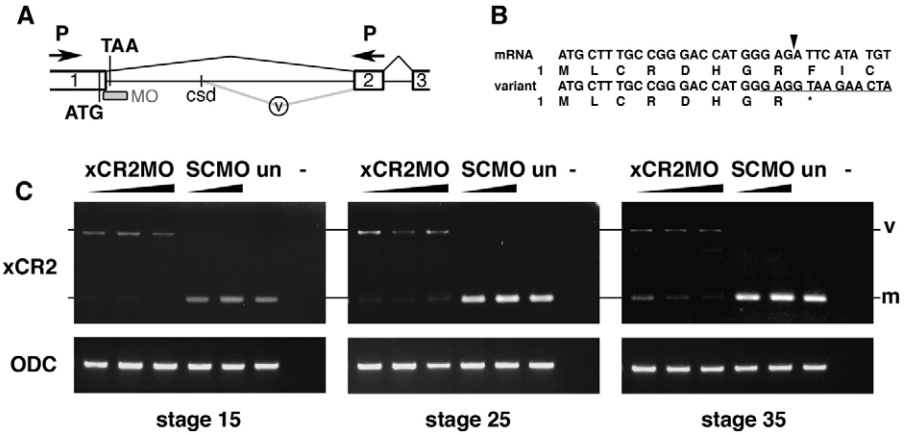

Fig. 4. XCR2 MO blocks endogenous RNA splicing. (**A**) Genomic structure including exon I (1), exon II (2), and exon III (3) of *XCR2*. The translation initiation codon (ATG) and a potential termination codon (TAA) are indicated. The splice-site-targeted antisense morpholino oligonucleotide XCR2 MO (MO) was designed against the sequence at the boundary of exon I/intron I. Abnormal splicing detected in XCR2 MO-injected embryos is shown by the gray line (v). The spliced variant is generated by a cryptic splice donor (csd) site 642 bp downstream from the end of exon I. (**B**) Sequence comparison of cDNA from mature mRNA and the aberrant splicing variant. Amino acid sequences are also indicated. The variant generated by abnormal splicing has a termination codon (correspondent to TAA in Fig. 4A) right after the end of exon I. Arrowhead indicates the correct exon I/exon II splice junction. The target sequence of XCR2 MO is underlined. (**C**) RT-PCR analyses of *XCR2* mRNA in XCR2 MO-injected embryos. Embryos were injected with 10, 20 and 50 ng of XCR2 MO, or 20 and 50 ng of Standard Control MO (SC MO), and harvested for RT-PCR at stage 15, 25 and 35. The primer set was designed to span the first intron to detect splicing of the endogenous *XCR2* pre-mRNA. In XCR2 MO-injected embryos, the mature mRNA (m) was decreased and an abnormal splicing variant (v) was detected. At stage 35, the mature *XCR2* mRNA was detectable at low levels in embryos injected with lowest dose (10 ng) of XCR2 MO.

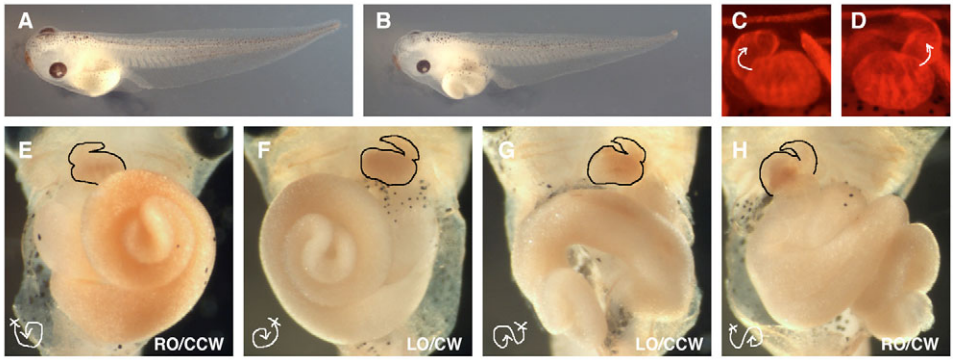

Fig. 5. XCR2 MO disturbs randomization of left-right asymmetric patterning of the heart and gut in stage 45-46 embryos. (**A**) Embryo injected with 50 ng of a standard control MO (SC MO). (**B**) Embryo injected with 50 ng of XCR2 MO. (**C-H**) Embryos injected with MO into the marginal region of both blastomeres at the two-cell stage, immunostained with MF 20 antibody, and the signal detected by fluorescence (C,D) or DAB staining (E-H). (C,E) Embryo injected with 50 ng of SC MO, showing normal left-right asymmetric patterning of the heart (C,E) and gut (right origin and counterclockwise coil, RO/CCW) (E). (D,F-H) Embryos injected with 20 ng of XCR2 MO. (D) Reversed morphology of heart. (F) Embryo has a mirror-imaged heart and gut (the left origin and clockwise coil, LO/CW). (G) Embryo has a normal heart, and left origin and counterclockwise-coiled gut (LO/CCW). (H) Embryo has reversed heart, right origin and clockwise-coiled gut (RO/CW).

We next examined the phenotype of XCR2 MO-injected embryos. The XCR2 MO did not cause any detectable defect in dorsoventral or anteroposterior axis patterning through stage 45, either in comparison to control MO-injected or uninjected embryos (Fig. 5A,B). There was also no effect of the XCR2 MO on movement or responsiveness of swimming tadpoles (data not shown). XCR2 MO-injected embryos were, however, extensively randomized with respect to left-right axis formation (Fig. 5C-H). The left-right patterning defects were scored according to Branford et al. (Branford et al., 2000); heart morphology is scored as normal or reversed, and gut morphology is scored for left or right origin of the gut, and for clockwise or counterclockwise coil direction. A low dose of XCR2 MO (20 ng) caused 23% reversed and 55% normal heart formation, 37% reversed and 41% normal gut origin, and 28% reversed and 50% normal gut coil direction (Table 1). A higher dose (50 ng) of XCR2 MO caused complete randomization of heart asymmetry (37% reversed and 39% normal). By contrast, 50 ng of the control MO had no significant effect on left-right patterning (90% and 89% normal heart and gut formation, respectively; Table 1).

XCR2 is expressed symmetrically in the lateral region at neurula stages (Fig. 2). This symmetric expression pattern is shared with other vertebrate EGF-CFC factors. EGF-CFC proteins are thought to be an essential component of a positive-feedback loop in which nodal-like ligands maintain and expand their own expression in the left lateral plate mesoderm (LPM) during the establishment of left-right axis patterning (Burdine and Schier, 2000; Hamada et al., 2002). The function of EGF-CFC proteins on the right side, however, has not been specifically addressed. To examine the role of *XCR2* in the left versus the right side of the embryo, embryos were injected XCR2 MO into one of two blastomeres after the first cleavage, which divides the embryo along the midline of the future left-right axis. Injection of 10 ng of XCR2 MO caused complete randomization of heart formation (48% reversed and 49% normal), and extensive, but incomplete, randomization of gut formation (23% mirror and 46% normal), when injected on the left side of the embryo (Table 2). By contrast, right-side injection did not affect left-right patterning, even at a dose of 20 ng of XCR2 MO (95% and 91% of normal heart and gut formation, respectively). These results indicate that left-side, but not right-side, expression of *XCR2* is necessary for the correct establishment of left-right asymmetry. We also examined left-side-specific expression of *XNR1* and *XATV* in the left LPM to establish whether *XCR2* is required in the left LPM for expression of these genes. Left-side injection of 10 ng of XCR2 MO inhibited *XNR1* expression in the LPM (84%), whereas right-side injection of XCR2 MO or left-side injection of control MO had no effect on *XNR1* expression (Fig. 6A-J, Table 3). Similarly, *XATV* expression in the left LPM was inhibited by left-side injection of 10 ng of XCR2 MO (90%), but the dorsal midline expression of *XATV* was not inhibited by *XCR2* depletion (Fig. 6O-R, Table 4).

The symmetric expression of *XNR1* has been reported to start before the left-right asymmetric expression of *XNR1* is detectable (Lohr et al., 1997; Lowe et al., 1996). We could first detect bilateral *XNR1* expression at stage 15 in two patches beside the presumptive notochord region, at the posterior of the archenteron roof (Fig. 7A-C), and left-side-specific *XNR1* expression began in the LPM at stage 20 (Fig. 7G,H, Table 8). Bilateral injection of

Table 1. The heart and gut morphology of XCR2 MO-injected embryos

	Amount of MO (ng)	Heart			Gut						
		Normal	Un	Mirror	Normal (RO/CCW)	RO/CW	Un	LO/CCW	Mirror (LO/CW)	Other	Total
Uninjected		95%	2%	0%	95%	1%	0%	1%	0%	3%	129
SC MO	20	85%	4%	6%	88%	3%	0%	4%	0%	4%	67
SC MO	50	90%	1%	1%	89%	3%	1%	0%	0%	7%	72
XCR2 MO	20	55%	4%	23%	27%	14%	4%	23%	14%	18%	56
XCR2 MO	50	39%	12%	37%	24%	22%	12%	18%	12%	12%	67

MOs were injected into the marginal region of both blastomeres at the two-cell stage. Embryos were counted at stage 45-46. Embryos which had other defects besides left-right axis (Other) were not counted in either heart and gut morphologies.
SC MO, standard control MO; Mirror, reversed left-right asymmetry; Un, undistinguishable left-right morphology; RO/CCW, right-origin/counterclockwise gut; RO/CW, right-origin/clockwise gut; LO/CCW, left-origin/counterclockwise gut; LO/CW, left-origin/clockwise gut; Other, other defects besides left-right axis.

Table 2. Left-side injection of XCR2 MO causes heart and gut asymmetry defects

	Amount of MO (ng)	Injection side	Heart			Gut						
			Normal	Un	Mirror	Normal (RO/CCW)	RO/CW	Un	LO/CCW	Mirror (LO/CW)	Other	Total
SC MO	10	Left	84%	5%	5%	84%	5%	0%	0%	5%	7%	43
SC MO	20	Left	96%	2%	2%	93%	4%	0%	2%	0%	0%	45
XCR2 MO	10	Left	49%	0%	48%	46%	15%	0%	14%	23%	2%	87
XCR2 MO	20	Left	39%	6%	52%	34%	19%	0%	15%	28%	3%	67
SC MO	10	Right	90%	0%	5%	90%	2%	0%	0%	2%	5%	41
SC MO	20	Right	98%	2%	0%	92%	8%	0%	0%	0%	0%	53
XCR2 MO	10	Right	99%	1%	0%	90%	3%	1%	4%	1%	0%	72
XCR2 MO	20	Right	95%	1%	0%	91%	3%	0%	1%	1%	4%	78

MOs were injected with 0.5-1.0 ng of *EGFP* RNA into the marginal region of one blastomere at the two-cell stage. Embryos were sorted by EGFP fluorescence at stage 20-21 and counted at stage 45-46. Embryos which had other defects besides left-right axis (Other) were not counted in either heart and gut morphologies.
SC MO, standard control MO; Mirror, left-right symmetry reversed; Un, undistinguishable left-right morphology; RO/CCW, right-origin/counterclockwise gut; RO/CW, right-origin/ clockwise gut; LO/CCW, left-origin/ counterclockwise gut; LO/CW, left-origin/clockwise gut; Other, other defects besides left-right axis.

XCR2 MO did not affect bilateral expression of *XNR1* at stage 15, before left-side-specific *XNR1* expression begins (Fig. 7E-F, Table 5). At stage 20, the initiation of expression of *XNR1* in the left-side LPM was efficiently inhibited by XCR2 MO, but the bilateral expression of *XNR1* was not affected (Fig. 7G-J, Table 5). Left-side-specific expression of *XNR1* was not detectable at stage 18 and 19 (data not shown). These observations indicate that at post-gastrula stages, bilateral posterior expression of *XNR1* is independent of XCR2, whereas left-side LPM specific expression is dependent on XCR2 at the earliest stage at which this expression can be detected.

To confirm the specificity of the effects of XCR2 MO on left-right asymmetric gene expression and visceral patterning, we examined whether ectopic expression of *XCR2* can rescue the defects caused by XCR2 MO, using a CMV promoter-driven *XCR2* expression plasmid (pCS-XCR2; Fig. 6D-R; Tables 3, 4). *XNR1* and *XATV* expression in the LPM were severely reduced in 84% or 90% of embryos, respectively, injected with 10 ng of XCR2 MO on the left side. *XNR1* and *XATV* expression in the LPM was restored in 86% or 45% of embryos co-injected with XCR2 MO and pCS-XCR2 plasmid on the left side. However, the spatial patterns of pCS-XCR2-rescued expression of *XNR1* were

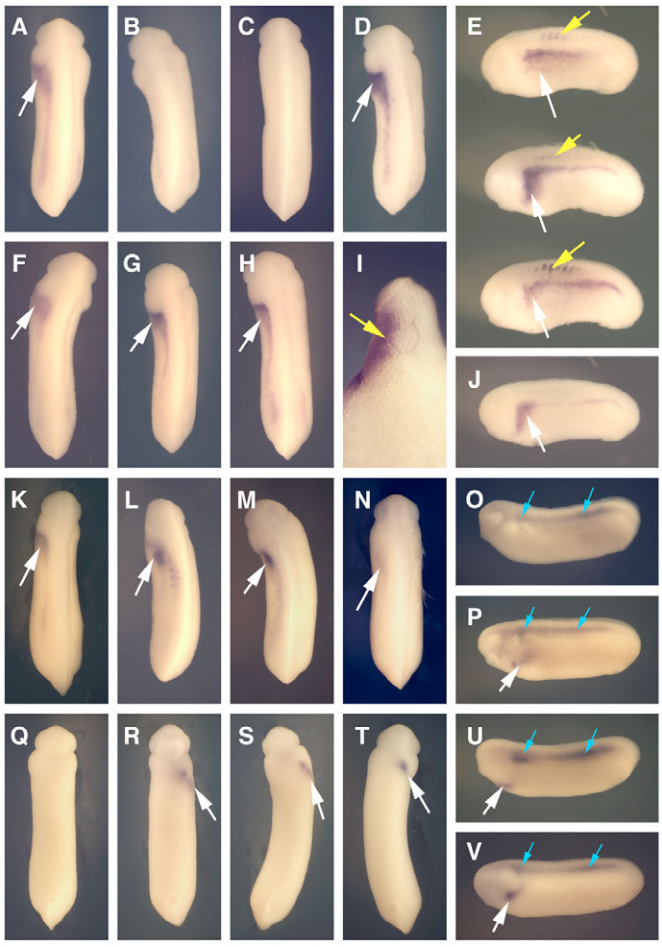

Fig. 6. Left-side injection of XCR2 MO inhibits *XNR1* and *XATV* expression in the lateral plate mesoderm (LPM). (**A-N**) In situ hybridization of *XNR1*. White arrows indicate the expression of *XNR1* in the LPM. (A) Embryo injected with 10 ng of SC MO into the left side, showing normal *XNR1* expression. (B) Injection of 10 ng of XCR2 MO into the left side caused no expression of *XNR1* in the LPM. (C) Co-injection of 10 ng of XCR2 MO with 10 pg of pCS-EGFP plasmid into the left side caused no expression of *XNR1* in the LPM. (D,E,I) Co-injection of 10 ng of XCR2 MO with 10 pg of pCS-XCR2 plasmid into the left side rescued the expression of *XNR1* in the LPM and also caused ectopic *XNR1* expression in the somite (yellow arrows). (I) Transverse section of the rescued embryo. Ectopic *XNR1* expression in the somite was observed. (F,G) Right-side injection of 10 ng of SC MO (F) or XCR2 MO (G) did not affect *XNR1* expression. (H,J) Uninjected control embryo. (K-N) Co-injection of 10 ng of XCR2 MO with 10 pg of *XCR1* (K), *XCR3S* (L), *XCR3L* (M) or human *CFC1* (N) plasmid in the left side rescued the expression of *XNR1* in the LPM. (**O-V**) In situ hybridization of *XATV* in ventral view. Arrows indicate the expression of *XATV* in the left LPM (white) and the dorsal midline (blue). (O,Q) Embryo injected with 10 ng of XCR2 MO in the left side inhibited the expression of *XATV* in the left LPM, but not in the dorsal midline. (P,R) Embryo injected with 10 ng of XCR2 MO in the right side, showing normal *XATV* expression. (S,U) Co-injection of 10 ng of XCR2 MO with 10 pg of pCS-XCR2 plasmid in the left side rescued the expression of *XATV* in the left LPM. (T,V) Uninjected control embryo.

Table 3. Rescue of XNR1 expression in XCR2-depleted lateral plate mesoderm (LPM) by EGF-CFC expression

	Amount of plasmid (pg)	Injection side	*XNR1* expression in the LPM: No signal	Left (normal)	Bilateral	Right (invert)	Total
SC MO	0	Left	0%	96%	4%	0%	25
SC MO+pCS-XCR2	10	Left	4%	96%	0%	0%	25
SC MO+pCS-XCR2	20	Left	0%	100%	0%	0%	24
SC MO+pCS-XCR2	40	Left	4%	88%	8%	0%	24
SC MO	0	Right	0%	96%	4%	0%	25
SC MO+pCS-XCR2	10	Right	4%	58%	29%	8%	24
SC MO+pCS-XCR2	20	Right	0%	72%	28%	0%	25
SC MO+pCS-XCR2	40	Right	4%	8%	36%	52%	25
XCR2 MO	0	Left	84%	12%*	0%	5%	57
XCR2 MO+pCS-XCR2	10	Left	0%	86%	14%	0%	44
XCR2 MO+pCS-XCR2	20	Left	16%	80%	4%	0%	25
XCR2 MO+pCS-XCR2	40	Left	12%	84%	4%	0%	25
XCR2 MO+pCS-XCR1	10	Left	7%	50%	26%	17%	42
XCR2 MO+pCS2-XCR3S	10	Left	14%	83%	3%	0%	35
XCR2 MO+pCS2-XCR3L	10	Left	9%	82%	9%	0%	33
XCR2 MO+pCS2-hCFC1	10	Left	11%	59%	22%	7%	27
XCR2 MO+pCS-EGFP	10	Left	88%	12%	0%	0%	42
XCR2 MO	0	Right	6%	92%	2%	0%	53
XCR2 MO+pCS-XCR2	10	Right	0%	32%	68%	0%	25
XCR2 MO+pCS-XCR2	20	Right	0%	39%	61%	0%	18
XCR2 MO+pCS-XCR2	40	Right	12%	28%	48%	12%	25

10 ng of MOs were injected with 0.5 ng of *EGFP* RNA and with various plasmids into the marginal region of one blastomere at the two-cell stage. Embryos were sorted by EGFP fluorescence at stage 20-21, fixed at stage 24-25 and prepared for analysis of *XNR1* expression by in situ hybridization.
SC MO, standard control MO.
*All embryos showed significantly reduced *XNR1* expression.

variable and often did not coincide well with the normal expression patterns of *XNR1* (Fig. 6E), which was consistent with the inability of plasmid injection to accurately recapitulate the spatial pattern, timing and dose of endogenous *XCR2* expression, confirmed by in situ hybridization of *XCR2* (data not shown). In addition, we examined the abilities of other *Xenopus* EGF-CFC members and human *CFC1* (*Cryptic*) to rescue the effect of the XCR2 MO. Co-injection with XCR2 MO and a CMV promoter-driven *XCR1*, *XCR3S*, *XCR3L* or human *CFC1* expression plasmid rescued *XNR1* expression in the LPM in 50%, 83%, 82% or 59% of embryos, respectively (Fig. 6K-N, Table 3). We also examined left-right asymmetric visceral patterning in tadpoles co-injected with pCS-XCR2 and the XCR2 MO. Co-injection of 10 pg of pCS-XCR2 rescued the left-right asymmetry of the heart and gut (73% and 80% of normal heart and gut formation, respectively; see Table 6). The efficiency of the rescue of morphological asymmetry was not improved by increasing the amount of injected *XCR2* plasmid (10, 20 and 40 pg). As in the case of the rescue of *XNR1* expression, this probably reflects the variable distribution of the rescue plasmid. These observations demonstrate, however, the specificity of action of the antisense MO, and also suggest a significant functional overlap among different members of the EGF-CFC family in their ability to participate in signaling during left-right patterning.

To determine whether *XCR2* may be limiting as well as necessary for nodal-family signaling during left-right patterning, we evaluated the effects of ectopic expression of *XCR2* by injection of pCS-XCR2. Right-side-specific injection of 10-40 pg of pCS-XCR2 with control MO causes significant perturbation of the asymmetric expression of *XNR1* relative to the left-side injection (Table 3). The right-side injection of pCS-XCR2 with control MO also caused abnormal heart and gut asymmetry (Table 6). Interestingly, right-side injection of 40 pg of pCS-XCR2 not only caused ectopic right-side expression of *XNR1* (38%), but also a significant number of reversals in the asymmetry of *XNR1* expression (52%) (Table 3). To investigate whether ectopic expression of *XCR2* on the right side is due to its function as a nodal/VG1 ligand co-receptor, we tested two mutants of *XCR2* in this assay: *XCR2 mEGF*, which is mutated in the EGF-like domain required for binding to nodal family ligands, and *XCR2 mCFC*, which is mutated in the CFC domain and no longer interacts with Type I nodal/VG1 receptors (Yeo and Whitman, 2001). In contrast to injection of wild-type *XCR2* on the

Table 4. The effect of *XCR2* depletion on expression of *XATV* in the lateral plate mesoderm (LPM)

	Amount of plasmid (pg)	Injection side	*XATV* expression in the LPM: No signal	Left (normal)	Bilateral	Right (invert)	Total
Uninjected	0		3%	97%	0%	0%	32
XCR2 MO	0	Left	90%	5%	0%	5%	39
XCR2 MO	0	Right	13%	87%	0%	0%	38
XCR2 MO+pCS-XCR2	10	Left	55%	45%	0%	0%	40

10 ng of MO was injected with 0.5 ng of *EGFP* RNA and with pCS-XCR2 plasmid into the marginal region of one blastomere at the two-cell stage. Embryos were sorted by EGFP fluorescence at stage 20-21, fixed at stage 26-27 and prepared for analysis of *XATV* expression by in situ hybridization.

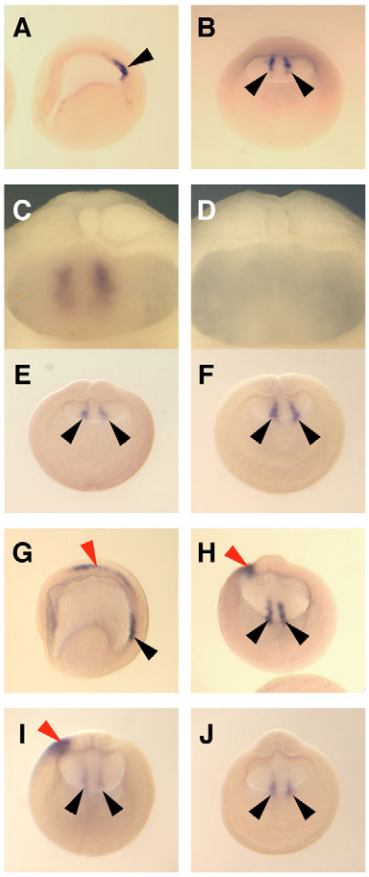

Fig. 7. Bilateral expression of *XNR1* is not affected by XCR2 MO injection. (**A-C**) Normal expression pattern of *XNR1* in the posterior archenteron roof at stage 15 as determined by in situ hybridization using uninjected embryos. Asymmetric expression of *XNR1* was not observed at stage 15. (C) Posterior archenteron roof of half-dissected embryo in side view. Two stripes of bilateral *XNR1* expression were observed. (**D**) In situ hybridization with an *XNR1* sense probe. No signal was observed in the archenteron roof. (**E**,**F**) Injection of 20 ng of SC MO (E) or of XCR2 MO (F) into the marginal region of both blastomeres at the two-cell stage. The bilateral expression of *XNR1* is not affected at stage 15 in either condition. (**G**,**H**) Normal expression pattern of *XNR1* at stage 20. The bilateral expression is maintained (black arrowheads) and asymmetric expression appears in the LPM (red arrowhead). (**I**) Injection of 20 ng of SC MO does not inhibit either bilateral or asymmetric expression of *XNR1* at stage 20. (**J**) Injection of 20 ng of XCR2 MO inhibited the asymmetric expression of *XNR1*, but not bilateral expression at stage 20. (A,G) Lateral views. The anterior side is to the left. (B,E,F,H-J) Posterior views. The dorsal side is up. The embryo was cleared with benzyl benzoate/benzyl alcohol (A,B,E-J). Black arrowheads indicate the bilateral expression of *XNR1*; red arrowheads indicate the asymmetric expression of *XNR1*.

right side, which caused ectopic *XNR1* expression in the right LPM and inhibited endogenous *XNR1* expression on the left side in 40% of embryos (Fig. 8B, Table 7), neither pCS-XCR2 mEGF nor pCS-XCR2 mCFC reversed the asymmetry in *XNR1* expression (Fig. 8A,C,D; Table 7). These results indicate that the ability of ectopic *XCR2* to change the left-side-specific *XNR1* expression depends on the function of XCR2 as a co-receptor for nodal/VG1 family ligands.

To clarify how right-side misexpression of *XCR2* causes left-right axis reversal, we examined the dynamics of *XNR1* and *XATV* expression in pCS-XCR2 injected embryos (Fig. 8, Tables 8, 9). Expression of *XNR1* or *XATV* in the right LPM following right-side injection of pCS-XCR2 was detectable by stage 15 in 17% (*XNR1*) or stage 17 in 45% (*XATV*) of injected embryos. This is in marked contrast to the normal expression of *XNR1* or *XATV* in the LPM, which is first detectable at stage 20 (*XNR1*) or at stage 23 (*XATV*) (Fig. 8G-K,M-Q; Tables 8, 9). In embryos injected on the right side with pCS-XCR2, endogenous left-side *XNR1* and *XATV* expression was absent at stage 20 in 67% (*XNR1*) and at stage 23 in 73% (*XATV*) of embryos, respectively. The endogenous expression of *XCR2* itself on the left side, however, was not affected by pCS-XCR2 injection on the right side (Fig. 8L,R). We also investigated whether the left-right asymmetry defect was overcome by *XNR1* misexpression on the left side, by using an EF1α promoter-driven *XNR1* expression plasmid (pXEX/*XNR1*) (Sampath et al., 1997). The heart and gut morphology was inverted by pCS-XCR2 injection into the right side in 57% and 46% of embryos, respectively (Table 10). Concomitant injection of 20 pg of pXEX/*XNR1* on the left side rescued the orientation of heart and gut morphology in 79% and 64% of injected embryos, whereas 20 pg of the pXEX control vector did not. This observation indicates that ectopic expression of XCR2 on the right is sufficient to initiate premature, ectopic expression of *XNR1* and *XATV* on the right side, leading to suppression of the normal expression of these factors on the left side.

Table 5. The effect of *XCR2* depletion on expression of *XNR1* in the posterior archenteron roof and in the LPM

		***XNR1* expression region**					
		Posterior archenteron roof	**LPM**				
	Stage	Bilateral	No signal	Left (normal)	Bilateral	Right (invert)	Total
SC MO	15	100%					25
XCR2 MO	15	100%					25
SC MO	20	100%	0%	92%	8%	0%	25
XCR2 MO	20	100%	100%	0%	0%	0%	26

20 ng of MOs were injected into the marginal region of both blastomeres at the two-cell stage. Embryos were fixed at stage 15 or 20, as indicated, and prepared for analysis of *XNR1* expression by in situ hybridization.
SC MO, standard control MO.

Table 6. CMV promoter-driven *XCR2* rescues the defects in heart and gut morphology caused by XCR2 MO

	Amount of MO (ng)	Injection side	Heart			Gut						
			Normal	Un	Mirror	Normal (RO/CCW)	RO/CW	Un	LO/CCW	Mirror (LO/CW)	Other	Total
SC MO	0	Left	95%	2%	0%	95%	2%	0%	0%	0%	2%	83
SC MO+pCS-XCR2	10	Left	91%	0%	6%	85%	6%	0%	6%	0%	3%	33
SC MO+pCS-XCR2	40	Left	73%	6%	21%	58%	21%	0%	8%	13%	0%	48
SC MO	0	Right	98%	1%	1%	90%	9%	1%	0%	0%	0%	87
SC MO+pCS-XCR2	10	Right	68%	8%	24%	76%	0%	0%	8%	16%	0%	25
SC MO+pCS-XCR2	40	Right	51%	2%	47%	31%	9%	0%	27%	33%	0%	55
XCR2 MO	0	Left	47%	3%	48%	46%	18%	0%	17%	17%	2%	94
XCR2 MO+pCS-XCR2	10	Left	73%	1%	25%	80%	1%	0%	13%	5%	1%	85
XCR2 MO+pCS-XCR2	20	Left	71%	0%	29%	84%	3%	0%	13%	0%	0%	38
XCR2 MO+pCS-XCR2	40	Left	75%	3%	23%	68%	25%	0%	8%	0%	0%	40
XCR2 MO	0	Right	97%	0%	0%	85%	7%	0%	4%	0%	3%	67
XCR2 MO+pCS-XCR2	10	Right	95%	2%	3%	89%	5%	0%	2%	5%	0%	62
XCR2 MO+pCS-XCR2	20	Right	100%	0%	0%	86%	6%	0%	3%	6%	0%	35
XCR2 MO+pCS-XCR2	40	Right	77%	0%	23%	51%	23%	0%	16%	9%	0%	43

10 ng of MOs were injected with 0.5 ng of *EGFP* RNA and with pCS-XCR2 plasmid into the marginal region of one blastomere at the two-cell stage. Embryos were sorted by EGFP fluorescence at stage 20-21 and scored at stage 45-46. Embryos, which had other defects besides left-right axis (Other), were not scored for heart and gut morphologies.
SC MO, standard control MO; Un, undistinguishable left-right morphology; RO/CCW, right-origin/counterclockwise gut; RO/CW, right-origin/clockwise gut; LO/CCW, left-origin/counterclockwise gut; LO/CW, left-origin/clockwise gut; Other, other defects besides left-right axis.

DISCUSSION

We report here the identification of three different EGF-CFC family members and examine the role of one of them, *XCR2*, in *Xenopus* embryogenesis. Our results, and those of K. Dorey and C. Hill (personal communication), suggest that all three are likely to be involved in mediating signaling by nodal-related ligands during embryogenesis. The spatially restricted expression patterns of frog EGF-CFC genes and their necessary role in nodal-related ligand signaling events, strongly suggest that the expression of these factors is locally limiting for signaling by nodal-related ligands in the post-gastrula embryo. Antisense morpholino-mediated loss-of-function experiments show that *XCR1* and *XCR3* are important for nodal-related signaling during pre-gastrula germ layer specification and patterning, whereas *XCR2* is specifically required for left-right patterning during neurula-tailbud stages, indicating that all three are likely to function as co-receptors (K. Dorey and C. Hill, personal communication). Although *XCR2* is expressed bilaterally on both sides of late neurulae, it is required only on the left side for correct patterning, consistent with a model in which nodal-related signaling on the left side of the LPM is required for left-side specification.

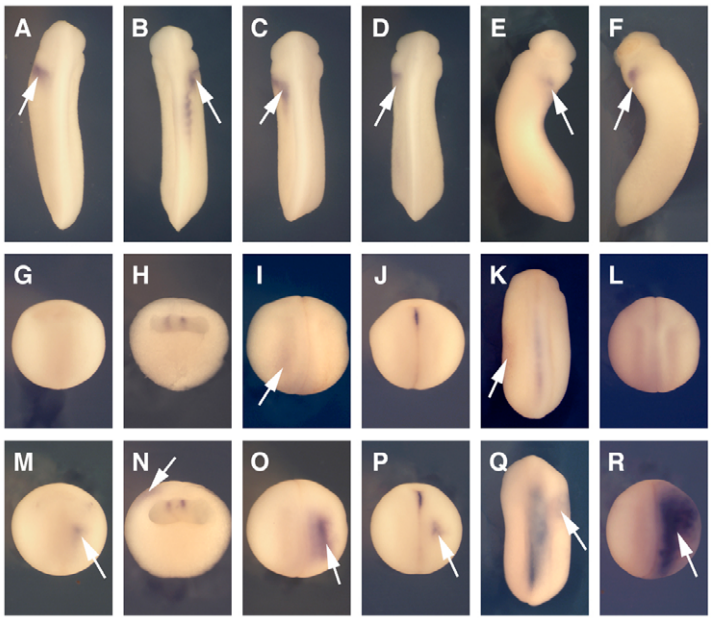

Fig. 8. Right-side overexpression of *XCR2* causes left-right inverted gene expression. (A-D,G-I,M-O) In situ hybridization of *XNR1* in dorsal view (A-D,G,I,M,O), anterior side at top, and in side view of a half-dissected embryo (H,N). (E,F,J,K,P,Q) In situ hybridization of *XATV* in ventral view (E,F) and in dorsal view (J-K,P,Q). (L,R) In situ hybridization of *XCR2* in dorsal view. (A,G-H) Embryo injected with 40 pg of pCS-EGFP plasmid in the right side. (B,M-R) Embryo injected with 40 pg of pCS-XCR2 into the right side. (**A**,**E**) Embryo showing normal expression of *XNR1* (A) or *XATV* (E) in the left LPM (arrow) at stage 25/26. (**B**,**F**) Right-side XCR2 overexpression caused right-side expression of *XNR1* (B) or *XATV* (F; arrow), and suppressed the left-side expression at stage 25/26. (**C**,**D**) Injection of 40 pg of pCS-XCR2 mEGF (C) or pCS-XCR2 mCFC (D) into the right side did not affect the expression pattern of *XNR1* (arrow) at stage 25. (**G**-**L**) Embryos injected with pCS-EGFP plasmid in the right side. *XNR1* expression was not detected in the LPM at stage 15 (G) and stage 16 (H), but was detectable at stage 20 (I) (arrow). *XATV* expression was not detected in the LPM at stage 17 (J), but was detectable at stage 23 (K; arrow). *XCR2* was expressed broadly at stage 20 (L). (**M**-**R**) Embryo injected with pCS-XCR2 plasmid in the right side. *XNR1* expression was ectopically expressed in the right LPM at stage 15 (M) and stage 16 (N), in addition to posterior bilateral expression. Strong *XNR1* expression was detected on the right side (arrow), but not on the left side at stage 20 (O). Ectopic *XATV* expression (arrow) was detected in the right LPM at stage 17 (P). *XATV* expression was detected on the right side (arrow), but not on the left side at stage 23 (Q). Left-side expression of *XCR2* was not affected, but very strong expression was detected on the right (injected) side at stage 20 (R).

Table 7. The expression of *XNR1* in the lateral plate mesoderm (LPM) following ectopic expression of wild-type or mutant *XCR2*

		XNR1 expression in the LPM				
	Injection side	No signal	Left (normal)	Bilateral	Right (invert)	Total
pCS-EGFP	Left	6%	94%	0%	0%	32
pCS-EGFP	Right	0%	100%	0%	0%	32
pCS-XCR2	Left	0%	92%	8%	0%	26
pCS-XCR2	Right	5%	0%	55%	40%	20
pCS-XCR2 mEGF	Left	0%	96%	4%	0%	25
pCS-XCR2 mEGF	Right	3%	97%	0%	0%	33
pCS-XCR2 mCFC	Left	0%	95%	5%	0%	20
pCS-XCR2 mCFC	Right	0	96%	4%	0	26

40 pg of plasmids were injected with 0.5 ng of *EGFP* RNA into the marginal region of one blastomere at the two-cell stage. Embryos were sorted by EGFP fluorescence at stage 20-21, fixed at stage 24-25 and analyzed for *XNR1* expression by in situ hybridization.

Table 8. Temporal analysis of expression of *XNR1* at the lateral plate mesoderm (LPM) following ectopic expression of *XCR2*

			XNR1 expression in the LPM				
	Injection side	Stage	No signal	Left (normal)	Bilateral	Right (invert)	Total
Uninjected		13/14	100%	0%	0%	0%	48
		15	100%	0%	0%	0%	24
		16/17	100%	0%	0%	0%	50
		18/19	100%	0%	0%	0%	58
		20	0%	100%	0%	0%	15
		21/22/23	2%	96%	2%	0%	56
		24/25	0%	100%	0%	0%	15
pCS-EGFP	Left	13/14	100%	0%	0%	0%	30
	Left	15	100%	0%	0%	0%	20
	Left	16/17	100%	0%	0%	0%	30
	Left	18/19	100%	0%	0%	0%	30
	Left	20	13%	80%	0%	7%	15
	Left	21/22/23	11%	95%	0%	0%	38
	Left	24/25	0%	100%	0%	0%	12
pCS-EGFP	Right	13/14	100%	0%	0%	0%	30
	Right	15	100%	0%	0%	0%	20
	Right	16/17	100%	0%	0%	0%	30
	Right	18/19	100%	0%	0%	0%	30
	Right	20	13%	88%	0%	0%	16
	Right	21/22/23	5%	93%	0%	2%	44
	Right	24/25	0%	90%	10%	0%	10
pCS-XCR2	Left	13/14	100%	0%	0%	0%	30
	Left	15	76%	24%	0%	0%	25
	Left	16/17	47%	53%	0%	0%	30
	Left	18/19	13%	87%	0%	0%	30
	Left	20	7%	93%	0%	0%	15
	Left	21/22/23	0%	96%	4%	0%	45
	Left	24/25	7%	93%	0%	0%	15
pCS-XCR2	Right	13/14	100%	0%	0%	0%	30
	Right	15	83%	0%	0%	17%	29
	Right	16/17	43%	0%	0%	57%	30
	Right	18/19	17%	0%	0%	83%	30
	Right	20	0%	7%	27%	67%	15
	Right	21/22/23	2%	4%	73%	20%	45
	Right	24/25	7%	20%	27%	47%	15

40 pg of plasmids were injected with 0.5 ng of *EGFP* RNA into the marginal region of one blastomere at the two-cell stage. Embryos were fixed at various stages and analyzed for *XNR1* expression by in situ hybridization.

Maintenance of localized expression of nodal ligands has been shown to depend on positive-feedback regulation mediated through a FAST1/FOXH1-responsive enhancer in the first intron of nodal orthologs in a broad range of chordate species (Whitman, 2001). Depletion of *XCR2* suppresses *XNR1* expression in the left-side LPM, consistent with a role for XCR2 as a co-factor in XNR1 signaling. The signals that initiate left-side-specific expression of *XNR1* in the frog embryo are not known. One possibility is that the posterior bilateral expression of *XNR1* is functionally comparable with *nodal* expression in the peri-nodal region of the mouse (Brennan et al., 2002; Saijoh et al., 2003), and that the *XNR1* signal from this posterior region is responsible for the initiation of *XNR1*

Table 9. Temporal analysis of expression of *XATV* at the lateral plate mesoderm (LPM) following ectopic expression of *XCR2*

			***XATV* expression in the LPM**				
	Injection side	Stage	No signal	Left (normal)	Bilateral	Right (invert)	Total
Uninjected		13/14	100%	0%	0%	0%	32
		15/16	100%	0%	0%	0%	34
		17	100%	0%	0%	0%	17
		18/19	100%	0%	0%	0%	33
		20/21/22	98%	2%	0%	0%	49
		23	12%	88%	0%	0%	17
		24/25	0%	100%	0%	0%	25
		26/27	0%	100%	0%	0%	29
pCS-EGFP	Left	13/14	100%	0%	0%	0%	30
	Left	15/16	100%	0%	0%	0%	30
	Left	17	100%	0%	0%	0%	25
	Left	18/19	100%	0%	0%	0%	30
	Left	20/21/22	100%	0%	0%	0%	45
	Left	23	20%	80%	0%	0%	20
	Left	24/25	7%	93%	0%	0%	15
	Left	26/27	0%	100%	0%	0%	15
pCS-EGFP	Right	13/14	100%	0%	0%	0%	30
	Right	15/16	100%	0%	0%	0%	30
	Right	17	100%	0%	0%	0%	25
	Right	18/19	100%	0%	0%	0%	30
	Right	20/21/22	100%	0%	0%	0%	45
	Right	23	7%	93%	0%	0%	15
	Right	24/25	0%	100%	0%	0%	15
	Right	26/27	8%	92%	0%	0%	13
pCS-XCR2	Left	13/14	100%	0%	0%	0%	30
	Left	15/16	100%	0%	0%	0%	30
	Left	17	60%	40%	0%	0%	25
	Left	18/19	43%	57%	0%	0%	30
	Left	20/21/22	40%	60%	0%	0%	45
	Left	23	23%	77%	0%	0%	35
	Left	24/25	13%	88%	0%	0%	40
	Left	26/27	10%	90%	0%	0%	20
pCS-XCR2	Right	13/14	100%	0%	0%	0%	30
	Right	15/16	100%	0%	0%	0%	30
	Right	17	55%	0%	0%	45%	29
	Right	18/19	47%	0%	0%	53%	30
	Right	20/21/22	49%	0%	0%	51%	45
	Right	23	20%	13%	13%	53%	30
	Right	24/25	17%	13%	20%	50%	30
	Right	26/27	24%	7%	0%	69%	29

40 pg of plasmids were injected with 0.5 ng of *EGFP* RNA into the marginal region of one blastomere at the two-cell stage. Embryos were fixed at various stages and analyzed for *XATV* expression by in situ hybridization.

expression in the left-side LPM through an XCR2-dependent pathway. A cilia-based mechanism for the left-right asymmetric distribution of nodal protein has been proposed (McGrath et al., 2003; Nonaka et al., 2002; Nonaka et al., 1998); whether a comparable mechanism might distribute the posterior-bilateral XNR1 asymmetrically is an interesting possibility, but it requires additional investigation. Alternatively, an asymmetric distribution of VG1 activity has been proposed as a mechanism for the initiation of left-right signaling (Chen et al., 2004; Hyatt et al., 1996; Kramer and Yost, 2002). This signal could also be dependent on XCR2 (alternatively it could depend on XCR1 and XCR3 (K. Dorey and C. Hill, personal communication), and therefore our data do not distinguish between these possibilities. We found that inhibition of XCR2 blocks left-side-specific expression of *XNR1* as early as this expression is detectable. Although we cannot rule out the possibility that a non-XCR2-dependent signal initiates left-side *XNR1* expression at a level not detectable by in situ hybridization, our data are consistent with the possibility that the initiation of asymmetric *XNR1* expression is XCR2 dependent. Once asymmetric *XNR1* expression is initiated, *XCR2* is also likely to be required for the activity of the FAST1/FOXH1-mediated positive-feedback loop maintaining *XNR1* expression in the left LPM.

The bilateral expression of *XNR1* in the posterior region of neurula stage embryos is not affected by depletion of *XCR2*. While it is possible that bilateral posterior expression is supported by residual *XCR2*, or by the perdurance of *XCR1* or *XCR3* from early embryogenesis, it seems likely that this expression is maintained by a mechanism distinct from the positive-feedback loop of *XNR1*. The pattern of *XCR2*-independent expression of *XNR1* is similar to the expression of mouse *Nodal* in the peri-nodal region, which is independent of *Cryptic* (Gaio et al., 1999; Yan et al., 1999), indicating a broad conservation of this posterior pattern of neurula-

Table 10. Left-side overexpression of *XNR1* rescues the heart and gut asymmetry defects induced by right-side overexpression of *XCR2*

		Heart			Gut						
Right-side injection	Left-side injection	Normal	Un	Mirror	Normal (RO/CCW)	RO/CW	Un	LO/CCW	Mirror (LO/CW)	Other	Total
None	None	99%	0%	0%	99%	0%	0%	0%	0%	1%	68
pCS-XCR2 40 pg	None	36%	2%	57%	25%	5%	0%	20%	46%	5%	61
pCS-XCR2 40 pg	pXEX vector 20 pg	53%	0%	42%	26%	5%	0%	3%	61%	5%	38
pCS-XCR2 40 pg	pXEX/*XNR1* 20 pg	79%	2%	10%	64%	10%	0%	0%	17%	10%	42

40 ng of pCS-XCR2 plasmid was injected with 0.5 ng of *EGFP* RNA into the marginal region of one blastomere at the two-cell stage, and then 20 pg of pXEX vector only or pXEX/*XNR1* plasmid was injected into the two left blastomeres at the four-cell stage. right-side EGFP-fluorescence-positive embryos were selected at stage 20-21 and counted at stage 45-46. Embryos which had other defects besides left-right axis (Other) were not counted in either heart and gut morphologies.
Mirror, reversed left-right asymmetry; Un, undistinguishable left-right morphology; RO/CCW, right-origin/counterclockwise gut; RO/CW, right-origin/clockwise gut; LO/CCW, left-origin/counterclockwise gut; LO/CW, left-origin/clockwise gut; Other, other defects besides left-right axis.

stage gene expression of nodal ligands among vertebrates. It is possible that this posterior bilateral expression of *XNR1* is transferred anteriorly in a left-right asymmetric manner to establish the asymmetric expression of *XNR1* in the LPM (Wright, 2001), but the basis for this transition to asymmetry remains unclear.

In contrast to effects on the left side LPM, depletion of *XCR2* on the right side of the embryo does not detectably alter left-right patterning. Although expression of both nodal family ligands and the nodal antagonists *lefty/antivin* is excluded from the right side (Branford et al., 2000; Cheng et al., 2000; Joseph and Melton, 1997; Lowe et al., 1996; Tanegashima et al., 2000), the extent or significance of their potential diffusion across and/or from the midline is not known. On the one hand, our results indicate that XCR2-dependent activity of neither the nodal family ligands nor their antagonists is essential on the right side for correct patterning. On the other hand, ectopic expression of *XCR2* is sufficient to reverse the left-right polarity, as can ectopic expression of TGFβ family ligands or activated receptors (Chen et al., 2004; Hanafusa et al., 2000; Hyatt et al., 1996; Sampath et al., 1997; Toyoizumi et al., 2000). Data from several laboratories, including our own, have shown that EGF-CFC proteins function as co-factors for nodal/GDF1 signaling, but are not sufficient to activate SMAD2 signaling in absence of the ligands (Fig. 3) (Saijo et al., 2000; Yan et al., 2002; Yeo and Whitman, 2001; Reissmann et al., 2001). That ectopic *XCR2* expression on the right side is enough to reverse left-right polarity indicates, therefore, that there are sufficient levels of nodal/GDF1 family ligands in the right-side LPM to initiate the left-side program when an exogenous co-receptor is provided. Ectopic *XCR2* is also sufficient to activate ectopic *XNR1* expression in the somites (Fig. 6), indicating that ectopic XCR2 can sensitize somites to endogenous nodal-related signals. This also suggests that the diffusion of XNR1 or related ligands is not restricted to the LPM at somite stages, although the possibility that nodal ligands are expressed at undetectable, but functionally significant, levels in the somite itself cannot be ruled out. Because left-side or right-side specific injections at the two-cell stage lead to variable expression in midline structures, our data do not distinguish a function for XCR2 expressed in midline structures such as the notochord in left-right patterning.

Why ectopic *XCR2* expression on the right is sufficient to flip the left-right orientation of *XNR1* expression remains an interesting theoretical question. This effect is eliminated by point mutations in either of the two domains required for XCR2 function as a nodal ligand co-receptor, strongly indicating that it is this function that mediates the observed effect on axis orientation. That ectopic *XCR2* expression is sufficient to reverse the polarity of *XNR1* expression suggests: (1) that XCR2 is limiting for activity of endogenous nodal/GDF1 family ligands on the right side of the embryo; (2) that elevated XCR2 enhances the activity of these ligands more than it enhances the activity of any lefty/antivin antagonists (Chen and Shen, 2004; Cheng et al., 2004; Tanegashima et al., 2004); (3) that the enhancement of activity of nodal/GDF1 ligands present on the right side is sufficient to establish a positive-feedback loop for *XNR1* expression in the right-side LPM; and (4) that this early *XNR1* expression on the right induces *XATV*, which in turn diffuses to suppress the normal activation of XNR1 signaling and expression on the left side.

The establishment of the left-right axis is a fascinating example of how an initial symmetry breaking event establishes a system of feedback loops that maintain a sharply divided asymmetry in the activity of a diffusible signaling molecule, in this case XNR1. Our observations suggest that XCR2 may be a critical limiting component of both the amplitude and the spatial extent of the left-side signal during left-right patterning. Consideration of this role for EGF-CFC factors will therefore be important for theoretical modeling of the dynamics of left-right patterning.

We thank Drs Marc Kirschner, Maximilian Muenke, Hazel Sive and Christopher V. E. Wright for gifts of plasmids; and the NIBB *Xenopus laevis* EST project and the American Type Culture Collection for EST clone resources. We thank Drs Caroline Hill and Karel Dorey for sharing results before publication. We thank Dr Michael Levin for helpful advice on photography. This work was supported by grants from the NICHD. C.-Y.Y. was supported by a grant (R08-2003-000-10943-0) from the Basic Research Program of the Korea Science & Engineering Foundation.

References

Adachi, H., Saijoh, Y., Mochida, K., Ohishi, S., Hashiguchi, H., Hirao, A. and Hamada, H. (1999). Determination of left/right asymmetric expression of nodal by a left side-specific enhancer with sequence similarity to a lefty-2 enhancer. *Genes Dev.* **13**, 1589-1600.
Adamson, E. D., Minchiotti, G. and Salomon, D. S. (2002). Cripto: a tumor growth factor and more. *J. Cell Physiol.* **190**, 267-278.
Altschul, S. F., Gish, W., Miller, W., Myers, E. W. and Lipman, D. J. (1990). Basic local alignment search tool. *J. Mol. Biol.* **215**, 403-410.
Bamford, R. N., Roessler, E., Burdine, R. D., Saplakoglu, U., dela Cruz, J., Splitt, M., Goodship, J. A., Towbin, J., Bowers, P., Ferrero, G. B. et al. (2000). Loss-of-function mutations in the EGF-CFC gene CFC1 are associated with human left-right laterality defects. *Nat. Genet.* **26**, 365-369.
Branford, W. W., Essner, J. J. and Yost, H. J. (2000). Regulation of gut and heart left-right asymmetry by context-dependent interactions between xenopus lefty and BMP4 signaling. *Dev. Biol.* **223**, 291-306.
Brennan, J., Norris, D. P. and Robertson, E. J. (2002). Nodal activity in the node governs left-right asymmetry. *Genes Dev.* **16**, 2339-2344.
Burdine, R. D. and Schier, A. F. (2000). Conserved and divergent mechanisms in left-right axis formation. *Genes Dev.* **14**, 763-776.
Chen, C. and Shen, M. M. (2004). Two modes by which Lefty proteins inhibit nodal signaling. *Curr. Biol.* **14**, 618-624.
Chen, X., Rubock, M. J. and Whitman, M. (1996). A transcriptional partner for MAD proteins in TGF-beta signalling. *Nature* **383**, 691-696.

Chen, Y., Mironova, E., Whitaker, L. L., Edwards, L., Yost, H. J. and Ramsdell, A. F. (2004). ALK4 functions as a receptor for multiple TGF beta-related ligands to regulate left-right axis determination and mesoderm induction in Xenopus. *Dev. Biol.* **268**, 280-294.
Cheng, A. M., Thisse, B., Thisse, C. and Wright, C. V. (2000). The lefty-related factor Xatv acts as a feedback inhibitor of nodal signaling in mesoderm induction and L-R axis development in xenopus. *Development* **127**, 1049-1061.
Cheng, S. K., Olale, F., Bennett, J. T., Brivanlou, A. H. and Schier, A. F. (2003). EGF-CFC proteins are essential coreceptors for the TGF-beta signals Vg1 and GDF1. *Genes Dev.* **17**, 31-36.
Cheng, S. K., Olale, F., Brivanlou, A. H. and Schier, A. F. (2004). Lefty Blocks a Subset of TGFbeta Signals by Antagonizing EGF-CFC Coreceptors. *PLoS Biol.* **2**, E30.
Ciccodicola, A., Dono, R., Obici, S., Simeone, A., Zollo, M. and Persico, M. G. (1989). Molecular characterization of a gene of the 'EGF family' expressed in undifferentiated human NTERA2 teratocarcinoma cells. *EMBO J.* **8**, 1987-1991.
Colas, J. F. and Schoenwolf, G. C. (2000). Subtractive hybridization identifies chick-cripto, a novel EGF-CFC ortholog expressed during gastrulation, neurulation and early cardiogenesis. *Gene* **255**, 205-217.
Ding, J., Yang, L., Yan, Y. T., Chen, A., Desai, N., Wynshaw-Boris, A. and Shen, M. M. (1998). Cripto is required for correct orientation of the anterior-posterior axis in the mouse embryo. *Nature* **395**, 702-707.
Dono, R., Montuori, N., Rocchi, M., De Ponti-Zilli, L., Ciccodicola, A. and Persico, M. G. (1991). Isolation and characterization of the CRIPTO autosomal gene and its X-linked related sequence. *Am. J. Hum. Genet.* **49**, 555-565.
Dono, R., Scalera, L., Pacifico, F., Acampora, D., Persico, M. G. and Simeone, A. (1993). The murine cripto gene: expression during mesoderm induction and early heart morphogenesis. *Development* **118**, 1157-1168.
Faure, S., Lee, M. A., Keller, T., ten Dijke, P. and Whitman, M. (2000). Endogenous patterns of TGFbeta superfamily signaling during early Xenopus development. *Development* **127**, 2917-2931.
Gaio, U., Schweickert, A., Fischer, A., Garratt, A. N., Muller, T., Ozcelik, C., Lankes, W., Strehle, M., Britsch, S., Blum, M. et al. (1999). A role of the cryptic gene in the correct establishment of the left-right axis. *Curr. Biol.* **9**, 1339-1342.
Gritsman, K., Zhang, J., Cheng, S., Heckscher, E., Talbot, W. S. and Schier, A. F. (1999). The EGF-CFC protein one-eyed pinhead is essential for nodal signaling. *Cell* **97**, 121-132.
Hamada, H., Meno, C., Watanabe, D. and Saijoh, Y. (2002). Establishment of vertebrate left-right asymmetry. *Nat. Rev. Genet.* **3**, 103-113.
Hanafusa, H., Masuyama, N., Kusakabe, M., Shibuya, H. and Nishida, E. (2000). The TGF-beta family member derriere is involved in regulation of the establishment of left-right asymmetry. *EMBO Rep.* **1**, 32-39.
Hyatt, B. A., Lohr, J. L. and Yost, H. J. (1996). Initiation of vertebrate left-right axis formation by maternal Vg1. *Nature* **384**, 62-65.
Joseph, E. M. and Melton, D. A. (1997). Xnr4: a Xenopus nodal-related gene expressed in the Spemann organizer. *Dev. Biol.* **184**, 367-372.
Kinoshita, N., Minshull, J. and Kirschner, M. W. (1995). The identification of two novel ligands of the FGF receptor by a yeast screening method and their activity in Xenopus development. *Cell* **83**, 621-630.
Kramer, K. L. and Yost, H. J. (2002). Ectodermal syndecan-2 mediates left-right axis formation in migrating mesoderm as a cell-nonautonomous Vg1 cofactor. *Dev. Cell* **2**, 115-124.
Lee, M. A., Heasman, J. and Whitman, M. (2001). Timing of endogenous activin-like signals and regional specification of the Xenopus embryo. *Development* **128**, 2939-2952.
Linask, K. K., Han, M. D., Linask, K. L., Schlange, T. and Brand, T. (2003). Effects of antisense misexpression of CFC on downstream flectin protein expression during heart looping. *Dev. Dyn.* **228**, 217-230.
Lohr, J. L., Danos, M. C. and Yost, H. J. (1997). Left-right asymmetry of a nodal-related gene is regulated by dorsoanterior midline structures during Xenopus development. *Development* **124**, 1465-1472.
Lowe, L. A., Supp, D. M., Sampath, K., Yokoyama, T., Wright, C. V., Potter, S. S., Overbeek, P. and Kuehn, M. R. (1996). Conserved left-right asymmetry of nodal expression and alterations in murine situs inversus. *Nature* **381**, 158-161.
Lustig, K. D., Kroll, K., Sun, E., Ramos, R., Elmendorf, H. and Kirschner, M. W. (1996). A Xenopus nodal-related gene that acts in synergy with noggin to induce complete secondary axis and notochord formation. *Development* **122**, 3275-3282.
McGrath, J., Somlo, S., Makova, S., Tian, X. and Brueckner, M. (2003). Two populations of node monocilia initiate left-right asymmetry in the mouse. *Cell* **114**, 61-73.
Minchiotti, G., Parisi, S., Liguori, G. L., D'Andrea, D. and Persico, M. G. (2002). Role of the EGF-CFC gene cripto in cell differentiation and embryo development. *Gene* **287**, 33-37.
Nieuwkoop, P. D. and Faber, J. (1956). *Normal Table of Xenopus laevis (Daudin)*. Amsterdam: North-Holland.
Nonaka, S., Tanaka, Y., Okada, Y., Takeda, S., Harada, A., Kanai, Y., Kido, M. and Hirokawa, N. (1998). Randomization of left-right asymmetry due to loss of nodal cilia generating leftward flow of extraembryonic fluid in mice lacking KIF3B motor protein. *Cell* **95**, 829-837.
Nonaka, S., Shiratori, H., Saijoh, Y. and Hamada, H. (2002). Determination of left-right patterning of the mouse embryo by artificial nodal flow. *Nature* **418**, 96-99.
Norris, D. P., Brennan, J., Bikoff, E. K. and Robertson, E. J. (2002). The Foxh1-dependent autoregulatory enhancer controls the level of Nodal signals in the mouse embryo. *Development* **129**, 3455-3468.
Osada, S. I., Saijoh, Y., Frisch, A., Yeo, C. Y., Adachi, H., Watanabe, M., Whitman, M., Hamada, H. and Wright, C. V. (2000). Activin/nodal responsiveness and asymmetric expression of a Xenopus nodal-related gene converge on a FAST-regulated module in intron 1. *Development* **127**, 2503-2514.
Reissmann, E., Jornvall, H., Blokzijl, A., Andersson, O., Chang, C., Minchiotti, G., Persico, M. G., Ibanez, C. F. and Brivanlou, A. H. (2001). The orphan receptor ALK7 and the Activin receptor ALK4 mediate signaling by Nodal proteins during vertebrate development. *Genes Dev.* **15**, 2010-2022.
Saijoh, Y., Adachi, H., Sakuma, R., Yeo, C. Y., Yashiro, K., Watanabe, M., Hashiguchi, H., Mochida, K., Ohishi, S., Kawabata, M. et al. (2000). Left-right asymmetric expression of lefty2 and nodal is induced by a signaling pathway that includes the transcription factor FAST2. *Mol. Cell* **5**, 35-47.
Saijoh, Y., Oki, S., Ohishi, S. and Hamada, H. (2003). Left-right patterning of the mouse lateral plate requires nodal produced in the node. *Dev. Biol.* **256**, 160-172.
Saloman, D. S., Bianco, C., Ebert, A. D., Khan, N. I., De Santis, M., Normanno, N., Wechselberger, C., Seno, M., Williams, K., Sanicola, M. et al. (2000). The EGF-CFC family: novel epidermal growth factor-related proteins in development and cancer. *Endocr. Relat. Cancer* **7**, 199-226.
Sambrook, J. and Russell, D. W. (2001). *Molecular Cloning: A Laboratory Guide*. New York: Cold Spring Harbor Laboratory Press.
Sampath, K., Cheng, A. M., Frisch, A. and Wright, C. V. (1997). Functional differences among Xenopus nodal-related genes in left-right axis determination. *Development* **124**, 3293-3302.
Schier, A. F. (2003). Nodal signaling in vertebrate development. *Annu. Rev. Cell Dev. Biol.* **19**, 589-621.
Schiffer, S. G., Foley, S., Kaffashan, A., Hronowski, X., Zichittella, A. E., Yeo, C. Y., Miatkowski, K., Adkins, H. B., Damon, B., Whitman, M. et al. (2001). Fucosylation of Cripto is required for its ability to facilitate nodal signaling. *J. Biol. Chem.* **276**, 37769-37778.
Schlange, T., Schnipkoweit, I., Andree, B., Ebert, A., Zile, M. H., Arnold, H. H. and Brand, T. (2001). Chick CFC controls Lefty1 expression in the embryonic midline and nodal expression in the lateral plate. *Dev. Biol.* **234**, 376-389.
Shen, M. M. and Schier, A. F. (2000). The EGF-CFC gene family in vertebrate development. *Trends Genet.* **16**, 303-309.
Shen, M. M., Wang, H. and Leder, P. (1997). A differential display strategy identifies Cryptic, a novel EGF-related gene expressed in the axial and lateral mesoderm during mouse gastrulation. *Development* **124**, 429-442.
Sive, H. L., Grainger, R. M. and Harland, R. M. (2000). *Early Development of Xenopus laevis: A Laboratory Manual*. New York: Cold Spring Harbor Laboratory Press.
Sun, B. I., Bush, S. M., Collins-Racie, L. A., LaVallie, E. R., DiBlasio-Smith, E. A., Wolfman, N. M., McCoy, J. M. and Sive, H. L. (1999). derriere: a TGF-beta family member required for posterior development in Xenopus. *Development* **126**, 1467-1482.
Tanegashima, K., Yokota, C., Takahashi, S. and Asashima, M. (2000). Expression cloning of Xantivin, a Xenopus lefty/antivin-related gene, involved in the regulation of activin signaling during mesoderm induction. *Mech. Dev.* **99**, 3-14.
Tanegashima, K., Haramoto, Y., Yokota, C., Takahashi, S. and Asashima, M. (2004). Xantivin suppresses the activity of EGF-CFC genes to regulate nodal signaling. *Int. J. Dev. Biol.* **48**, 275-283.
Tao, Q., Yokota, C., Puck, H., Kofron, M., Birsoy, B., Yan, D., Asashima, M., Wylie, C. C., Lin, X. and Heasman, J. (2005). Maternal wnt11 activates the canonical wnt signaling pathway required for axis formation in Xenopus embryos. *Cell* **120**, 857-871.
Toyoizumi, R., Mogi, K. and Takeuchi, S. (2000). More than 95% reversal of left-right axis induced by right-sided hypodermic microinjection of activin into Xenopus neurula embryos. *Dev. Biol.* **221**, 321-336.
Watanabe, M. and Whitman, M. (1999). FAST-1 is a key maternal effector of mesoderm inducers in the early Xenopus embryo. *Development* **126**, 5621-5634.
Weisberg, E., Winnier, G. E., Chen, X., Farnsworth, C. L., Hogan, B. L. and Whitman, M. (1998). A mouse homologue of FAST-1 transduces TGF beta superfamily signals and is expressed during early embryogenesis. *Mech. Dev.* **79**, 17-27.
Wessely, O., Kim, J. I., Geissert, D., Tran, U. and De Robertis, E. M. (2004). Analysis of Spemann organizer formation in Xenopus embryos by cDNA macroarrays. *Dev. Biol.* **269**, 552-566.

Whitman, M. (2001). Nodal signaling in early vertebrate embryos: themes and variations. *Dev. Cell* **1**, 605-617.
Wright, C. V. (2001). Mechanisms of left-right asymmetry: what's right and what's left? *Dev. Cell* **1**, 179-186.
Xu, C., Liguori, G., Persico, M. G. and Adamson, E. D. (1999). Abrogation of the Cripto gene in mouse leads to failure of postgastrulation morphogenesis and lack of differentiation of cardiomyocytes. *Development* **126**, 483-494.
Yabe, S., Tanegashima, K., Haramoto, Y., Takahashi, S., Fujii, T., Kozuma, S., Taketani, Y. and Asashima, M. (2003). FRL-1, a member of the EGF-CFC family, is essential for neural differentiation in Xenopus early development. *Development* **130**, 2071-2081.
Yan, Y. T., Gritsman, K., Ding, J., Burdine, R. D., Corrales, J. D., Price, S. M., Talbot, W. S., Schier, A. F. and Shen, M. M. (1999). Conserved requirement for EGF-CFC genes in vertebrate left-right axis formation. *Genes Dev.* **13**, 2527-2537.
Yan, Y. T., Liu, J. J., Luo, Y., Chaosu, E., Haltiwanger, R. S., Abate-Shen, C. and Shen, M. M. (2002). Dual roles of Cripto as a ligand and coreceptor in the nodal signaling pathway. *Mol. Cell. Biol.* **22**, 4439-4449.
Yeo, C. and Whitman, M. (2001). Nodal signals to Smads through Cripto-dependent and Cripto-independent mechanisms. *Mol. Cell* **7**, 949-957.
Zhang, J., Talbot, W. S. and Schier, A. F. (1998). Positional cloning identifies zebrafish one-eyed pinhead as a permissive EGF-related ligand required during gastrulation. *Cell* **92**, 241-251.